Activation Barriers for Addition of Methyl Radicals to Oxygen-Stabilized Carbocations

John C. Traeger[†] and Thomas Hellman Morton*[,‡]

Department of Chemistry, La Trobe University, Bundoora, Victoria, Australia 3086, and Department of Chemistry, University of California, Riverside, California 92521-0403

Received: May 26, 2005; In Final Form: August 11, 2005

Activation barriers ($\Delta H_{Me}^{\ddagger}$) for adding methyl radicals to ions of the general formula $CH_3CR{=}OCH_3^+$ have been measured by looking at the threshold energies for the reverse reaction, dissociative photoionization of ethers of the general formula $RC(CH_3)_2OCH_3$. Dissociation by loss of a methyl radical has more favorable thermochemistry than loss of R$^\bullet$, yet the onset of R$^\bullet$ loss occurs at lower energies than loss of $CH_3^\bullet$. In other words, the more endothermic dissociation exhibits a lower appearance energy. Contrathermodynamic ordering of appearance energies is observed for R = Et, *n*Pr, *i*Pr, *t*Bu, and neopentyl. The sum of the appearance energy difference, ΔAE, and the thermochemical difference ($\Delta\Delta H$, calculated using G3 theory) gives a lower bound for the barrier for adding methyl radical to $CH_3CR{=}OCH_3^+$. More specifically, the difference between that activation barrier and the one for adding R$^\bullet$ to $(CH_3)_2C{=}OCH_3^+$, $\Delta H_{Me}^{\ddagger} - \Delta H_R^{\ddagger}$, equals $\Delta AE + \Delta\Delta H$ and has values in the range 20−24 kJ mol^{-1} for the homologous series investigated. There is no systematic trend with the steric bulk of R, and available evidence suggests that $\Delta H_R^{\ddagger}$ does not have a value >5 kJ mol^{-1}. The difference in barrier heights, $\Delta H_{Me}^{\ddagger} - \Delta H_{iPr}^{\ddagger}$ for $CH_3^\bullet$ plus $iPrC(CH_3){=}OX^+$ vs $iPr^\bullet + (CH_3)_2C{=}OX^+$, has the same value, regardless of whether X = H or CH_3. Mixing of higher energy electronic configurations provides a qualitative theoretical explanation for some (but not all) observed trends in barrier heights.

Introduction

Methyl radicals are among the most reactive transient species encountered in chemical reactions. The approach of two alkyl radicals to form a carbon−carbon single bond is widely believed to be barrier free, so long as the reactants have no net angular momentum.[1] Similarly, theory predicts that the addition of a methyl radical to a methyl cation (to form ionized ethane),[2] to an ethyl cation (to form ionized propane),[3] or to an isopropyl cation (to form ionized isobutane)[4] also takes place without potential energy barriers. By contrast, it has been known for half a century that methyl radicals encounter significant activation barriers when adding to carbon−carbon double bonds to form larger alkyl radicals.[5] For example, attack of the more substituted end of the double bond of isobutene by methyl radical to form neopentyl radical has an activation energy of $\Delta H^{\ddagger} = 44$ kJ mol^{-1},[6] within experimental error of the value predicted by ab initio calculations, 41 kJ mol^{-1}.[7] Equation 1 represents this reaction, where R = methyl and X stands for an sp^2-hybridized CH_2 group.

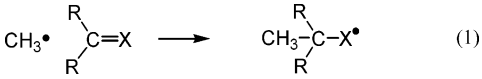

(1)

This paper reports experimental determinations of the barriers for addition of methyl radicals to oxygen-stabilized carbocations, in which the group X corresponds to a charged methoxy group (OCH_3^+). In terms of resonance theory, a lone pair on the oxygen donates electron density to the vacant *p* orbital of an adjacent cationic center, conferring a high degree of π-character to the carbon−oxygen bond. Equation 2 depicts that variant of eq 1 more explicitly, where $\Delta H_{Me}^{\ddagger}$ stands for the activation energy of the addition.

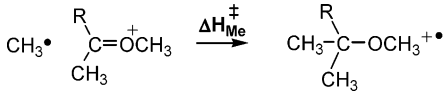

(2)

As first pointed out nearly two decades ago by Hammerum and Derrick[8] in the case of $X = NH_2^+$, a barrier exists for addition of a methyl radical to the sp^2 carbon. They observed that carbon−carbon bond cleavage in *tert*-butylamine radical cation, $(CH_3)_3CNH_2^{+\bullet}$, must have an energy barrier for the reverse reaction, since the metastable ion decomposition of $(CH_3)_3CNH_2^{+\bullet}$ displays a large kinetic energy release for methyl loss. In other words, addition of methyl radical to the $(CH_3)_2C{=}NH_2^+$ ion has to surmount a potential energy maximum.

By extension, one would suspect that radical cations from *tert*-alcohols and their ethers might also encounter barriers to dissociation that exceed the thermodynamic threshold. Such is the prediction of ab initio calculations on carbon−carbon bond cleavage in methyl *tert*-butyl ether.[9] An experimental test cannot be performed by the method of Hammerum and Derrick, however, since the molecular ion intensities from saturated tertiary alcohols and ethers are far too weak for their metastable ion decompositions to be observed in a conventional double-focusing mass spectrometer. The present work explores an alternative approach for studying energy barriers, namely, by examining differences in appearance energies for competing unimolecular decompositions.

A number of *tert*-alkyl ethers are used as antiknock agents in gasoline and are known by their acronyms, such as MTBE

* To whom correspondence may be addressed. E-mail: morton@ucrac1.ucr.edu.
† La Trobe University.
‡ University of California, Riverside.

10.1021/jp052790a CCC: $30.25
Published on Web 10/22/2005

(methyl *tert*-butyl ether, R═CH_3). These include TAME (*tert*-amyl methyl ether, **1**, R═CH_3CH_2) and TOME (*tert*-octyl methyl ether, **5**, R = $(CH_3)_3CCH_2$). This investigation looks at the homologous series **1**−**5**, along with selected homologues and deuterated analogues.

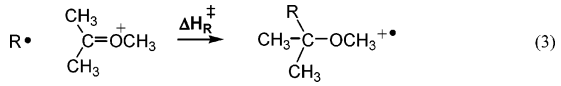

(3)

The activation energy $\Delta H_{Me}^{\ddagger}$ is measured relative to the activation barrier $\Delta H_R^{\ddagger}$ for addition of a larger radical R to the $(CH_3)_2C{=}OCH_3^+$ ion, as illustrated in eq 3. Equations 2 and 3 produce the same radical cations. In determining the threshold energies for the dissociations corresponding to the reverse of eqs 2 and 3, we have previously noted that the thermodynamically most favorable cleavage has a higher appearance energy than the less favorable one.[10] The contrast between thermochemical expectations and observed onsets provides experimental evidence of an activation barrier for eq 2. In combination with theoretical estimates of relative stabilities, the experimental data provide lower bounds for $\Delta H_{Me}^{\ddagger}$ for the homologous series R = ethyl, *n*-propyl, isopropyl, *tert*-butyl, and neopentyl.

Experimental Section

TAME (**1**) was purchased from Aldrich and used without further purification. Except where otherwise specified, the other methyl *tert*-alkyl ethers were prepared by converting the corresponding alcohols to their alkoxides by refluxing with sodium hydride in THF, followed by addition of an excess of iodomethane and further reflux. All synthesized ethers were purified by two successive distillations at atmospheric pressure, the second one from lithium aluminum hydride to remove unreacted alcohol and other active hydrogen impurities.

1,1,1-Trifluoro-2-methyl-2-butanol was prepared as described in the literature[11] and purified by distillation. **2-methyl-2-methoxybutane-4-*d*$_1$ (1-*d*$_1$)** was prepared from commercially available 3-methoxy-3-methyl-1-butanol (Aldrich) by conversion to the corresponding tosylate and reduction with lithium aluminum deuteride. **2-Methoxy-2-methylpentane (2**) was prepared from the corresponding commercially available alcohol, 2-methyl-2-pentanol (Avocado Research Chemicals, Ltd.), as described above. **3-Methoxy-3-ethylhexane (6**) was prepared from the commercial alcohol, 3-ethyl-3-hexanol (Avocado Research Chemicals, Ltd.), as described above. **3-Methoxy-3-methyl-*d*$_3$-hexane** (**7**) was prepared by addition of methyl-d_3 magnesium iodide (Aldrich) to 3-hexanone, followed by distillation of the resulting alcohol and conversion to the methyl ether as described above. **2-Methoxy-2,3-dimethylbutane (methyl *tert*-hexyl ether, 3)** was prepared from commercially available 2,3-dimethyl-2-butanol (Aldrich) as described above. The d_6 analogue of that alcohol was prepared by addition of isobutyryl chloride (Aldrich) to excess methyl-d_3 magnesium iodide (Aldrich) and converted to the corresponding ether, **2-methoxy-2,3-dimethylbutane-*d*$_6$ (3-*d*$_6$)**, as described above. The 70-eV mass spectrum of this d_6 analogue of **3** exhibits *m*/*z* 79 (loss of isopropyl radical) as the most abundant fragment and *m*/*z* 46 as the next most intense peak. At high resolution, the *m*/*z* 46 is found to consist of two isobaric ions of comparable intensity, separated by 0.033 amu. Exact mass measurements show these to be CD_3CO^+ and $C_3D_5^+$ ions, an assignment confirmed by the fact that the 70-eV mass spectrum of *tert*-butanol-d_6 exhibits the same pair of isobaric ions, with a measured separation of 0.034 amu. **2-Methoxy-2,3,3-trimethylbutane-*d*$_6$ (MTMB-*d*$_6$, 4-*d*$_6$)** was prepared by addition of excess acetone-d_6 (Acros) to a pentane solution of *tert*-butyllithium (Acros) at −78 °C followed by distillation of the recovered alcohol and conversion to the methyl ether as described above. **2-Methoxy-*d*$_3$-2,4,4-trimethylpentane (5-*d*$_3$)** was prepared by the acid-catalyzed addition of methanol-d_3 to 2,4,4-trimethylpentane, as previously described for the unlabeled analogue.[10] ^{2}H NMR spectra were recorded at 76.77 MHz on a General Electric GN-500 instrument.

Photoionization efficiency curves were measured on an apparatus that has been described elsewhere.[12−14] The source of a microcomputer-controlled magnetic sector mass spectrometer makes use of the hydrogen pseudocontinuum and a Seya-Namioka monochromator equipped with a holographically ruled diffraction grating. Resolution of the monochromator was fixed at 1.35Å, and the absolute energy scale was internally calibrated with known reference emission lines to an accuracy of better than 0.001 eV. All experiments were performed at ambient temperature with sample pressures of 10^{-3} Pa in the ion-source region. The 298 K appearance energies (AEs) were obtained from a simple linear extrapolation of the PIE curves to zero ion current in the threshold region. AEs were adjusted to 0 K using unscaled vibrational frequencies computed at B3LYP/6-31G**, as described previously.[14] The uncertainties in AE differences (ΔAE values) are ±0.01 eV.

Calculations using density functional theory (DFT) and G3 theory were run using the GAUSSIAN98 and GAUSSIAN03 (Gaussian Inc.) program suites. Vertical triplet energies and vertical neutralization energies were calculated at B3LYP/6-31G** using geometries optimized for the corresponding ions. Thermochemical calculations for neutral ethers and ground state ions were performed at both G3 (which uses MP2/6-31G* optimized geometries) and G3//B3LYP (which uses B3LYP/6-31G* optimized geometries and is commonly abbreviated G3B3),[15] methods that have been shown to be effective for cation and for radical thermochemistries.[16] The difference between G3 and G3B3 results is taken to represent the uncertainty of theoretical thermochemical estimates. Topological analyses of electron densities were performed by the Atoms in Molecules approach[17] using AIM2000 (SBK Software). AIM bond orders have been conventionally defined as $n = e^{C(\rho-\rho_o)}$, where ρ represents the electron density at the bond critical point and ρ_o the electron density for a referenced single bond.[17] As we have elsewhere noted, this definition does not give a bond order $n = 0$ for $\rho = 0$.[18] Therefore, we redefine the AIM bond order as $n = e^{A(\rho-B)} - e^{-AB}$, where A and B are determined based on referenced single and double bonds.[17] For B3LYP/6-31G** wave functions, the constant C for carbon−oxygen bonds equals 4.94, while the constants A and B have values of 3.25 and 0.0952, respectively. For MP2(full) wave functions, the corresponding constants are $C = 5.33$, $A = 3.75$, and $B = 0.138$. The two alternative ways to calculate bond order do not give values very different from one another for the compounds under discussion here. For example, the C−OMe DFT bond orders for neutral *tert*-alkyl methyl ethers are $n = 0.91$ and 0.89, respectively, for the two alternative definitions. For oxygen-stabilized carbocations, the A/B parametrization gives values of n that are 0.03 greater than does the C/ρ_o parametrization. Both parametrizations give bond orders of 1.5 for the methoxy oxygen−carbon bond of RCMe═OMe^+ ions and 1.6 for the hydroxy-carbon bond of $CF_3CMe{=}OH^+$.

To calibrate computational estimates of thermochemistry, the adiabatic ionization energy (IE) of 2,2-dimethylbutane was measured experimentally and compared to the predictions of G3-level calculations. The experimental IE has the value 9.82

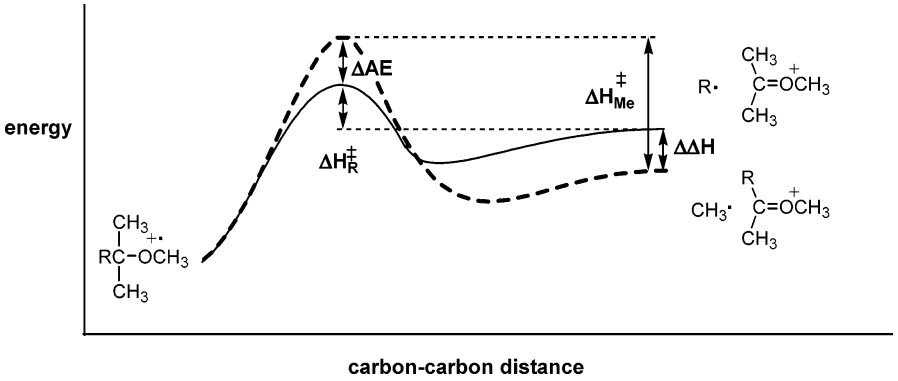

Figure 1. Schematic representation of potential-energy curves for competing dissociation pathways of radical cations of *tert*-alkyl methyl ethers, illustrating that the barrier for addition of a methyl radical to $RC(CH_3)=OCH_3^+$ ($\Delta H_{Me}^{\ddagger}$) is equal to the sum of the difference in appearance energies (ΔAE), the thermodynamic enthalpy difference ($\Delta\Delta H$), and the barrier for addition of R$^\bullet$ to $(CH_3)_2C=OCH_3^+$ ($\Delta H_R^{\ddagger}$).

$\pm$ 0.01 eV (assuming that the observed onset for the weak parent ion signal does not represent a hot band). No other experimental value has been published; the closest comparison is the adiabatic IE reported for the isomer 2,3-dimethylbutane (9.79 eV) based on charge-exchange equilibria.[19] The G3 value, 9.764 eV, and the G3B3 value, 9.768 eV, for 2,2-dimethylbutane are taken as the differences between the respective 0 K energies of the neutral and the geometry-optimized radical cation. Both geometry-optimized structures have C_s symmetry, but the radical cation is calculated to have an elongated C2−C3 bond, 1.98 Å at MP2/6-31G* and 2.11 Å at B3LYP/6-31G*. The large difference between neutral (C−C = 1.55Å) and ion geometries suggests that this comparison between experiment and theory comes close to a worst-case scenario. Thus, the accuracy of calculated ion energies is taken to be the 5 kJ mol^{-1} difference between experiment and theory for 2,2-dimethylbutane.

Results

This work was prompted by the observation that photoionization thresholds for competing bond cleavages do not always reflect the difference in reaction endothermicities. Figure 1 illustrates the logic of this investigation. Addition of an alkyl radical to an oxygen-stabilized carbocation produces a radical cation, as eqs 2 and 3 depict above. The reverse reaction corresponds to the dissociation of that radical cation, as Figure 1 depicts going from left to right. If the radical cation has competing dissociation pathways, the appearance energies (AEs) reflect not only their relative thermochemistry but also any intervening energy barriers. The difference between AEs for competing ion decompositions represents the difference in barrier heights, regardless of whether the reaction is viewed from left to right (dissociation) or right to left (addition of a radical to an oxygen-stabilized cation).

Equation 4 illustrates the competition in a tertiary alcohol, where the photon energies $h\nu_1$ and $h\nu_2$ stand for the observed onsets of the respective dissociations. Recently we reported photoionization efficiency curves for 2,3-dimethyl-2-butanol (thexyl alcohol: R = isopropyl and X = H) and noted that loss of the isopropyl radical has an AE *lower* than loss of a methyl radical, $h\nu_1 - h\nu_2 = 0.07$ eV.[18] The observed onset energies at which competing dissociations occur contrast with G3 calculations performed in the present study, which predict that the thermochemical threshold for loss of the larger radical ought to be 0.15 eV *higher* than for the smaller one. The difference between observed and thermochemical thresholds signifies that methyl loss has an activation energy in excess of its endothermicity. By microscopic reversibility, this difference represents the lower limit of the barrier for adding methyl radical to the protonated ketone (analogous to $\Delta H_{Me}^{\ddagger}$ in eq 2).

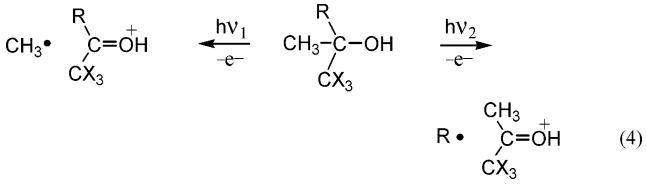

(4)

The question arises whether methyl losses always have higher AEs than losses of larger radicals. To address that issue, two compounds were examined, where it turns out that methyl loss does not have a higher AE than ethyl loss. According to the literature, 2,2-dimethylbutane exhibits an AE for methyl loss lower than the AE for ethyl loss.[20] In that hydrocarbon (as well as the oxygen-containing compounds reported below), alkane expulsions have appearance energies that are substantially lower than those for associated alkyl radical losses. This means the ^{13}C natural abundance peaks from methane and ethane loss from the ionized hydrocarbon overlap with the peaks from methyl and ethyl loss from precursors that contain only ^{12}C. Because the published photoionization curves do not appear to have been corrected for this effect, photoionization efficiencies for 2,2-dimethylbutane were reexamined. After correction for ^{13}C, the onset curves for methyl loss and ethyl loss were found to be virtually superimposable.

Trifluorinated *tert*-amyl alcohol (1,1,1-trifluoro-2-methyl-2-butanol: R = ethyl and X = F in eq 4) provides a more clear-cut example of a *tert*-alkyl system for which the thermodynamically more favorable fragmentation exhibits a lower AE. At 298 K, the AEs are 10.83 eV for methyl loss and 10.94 eV for ethyl loss. Theoretical calculations predict the thermochemical AE for methyl loss to be 11.065 eV (G3) or 11.067 eV (G3B3) at 0 K. When corrected to 0 K, the experimental AE for methyl loss is 11.06 eV. The AE for ethyl loss, $h\nu_2 - h\nu_1 = 0.11$ eV *higher* than for methyl loss, can be compared with the predicted thermochemical AE values, 11.221 eV (G3) and 11.213 eV (G3B3). While the difference in experimental AE values is not quite as great as the difference between thermodynamic thresholds predicted by G3 (0.156 eV) or G3B3 (0.146 eV) calculations, the experimental result demonstrates that methyl loss from a tertiary alcohol does not always have a higher AE than loss of a larger radical. Parenthetically, it should be noted that G3 and G3B3 calculations predict a 0 K AE for CF_3 loss of 10.35 eV. The difference between this and the experimental value (10.66 eV at 298 K, which converts to 10.89 eV

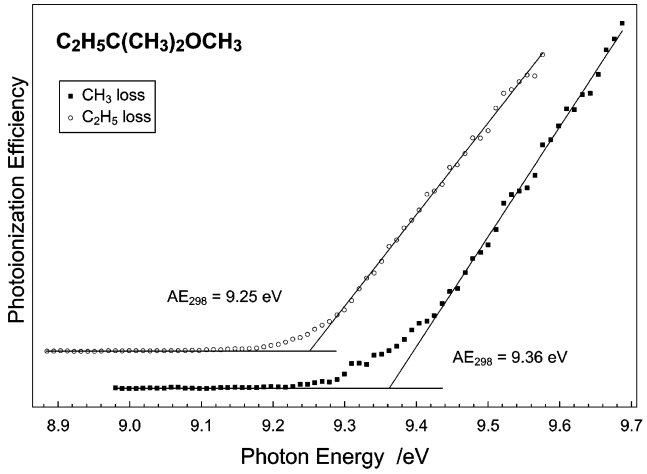

Figure 2. Photoionization efficiency curves near onset for loss of methyl radical (*m*/*z* 87) and for loss of ethyl radical (*m*/*z* 73) from TAME (**1**) showing 298 K appearance energies. The observed 298 K threshold for loss of ethane is 9.15 eV.

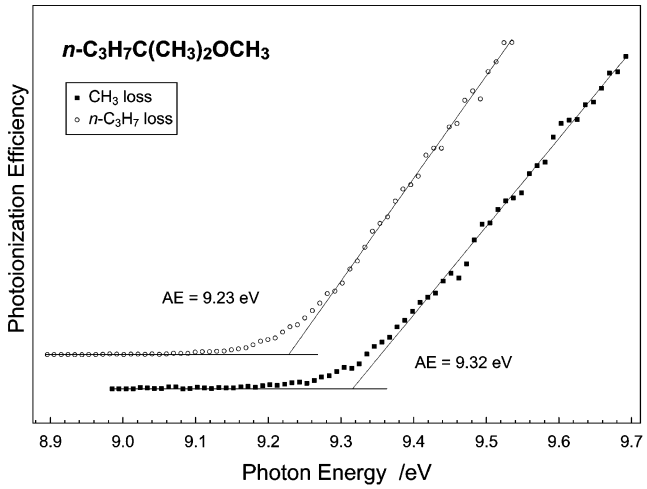

Figure 3. Photoionization efficiency curves near onset for loss of methyl radical (*m*/*z* 101) and for loss of C_3H_7 radical (*m*/*z* 73) from **2** showing 298 K appearance energies. The observed 298 K threshold for loss of propane is 9.13 eV.

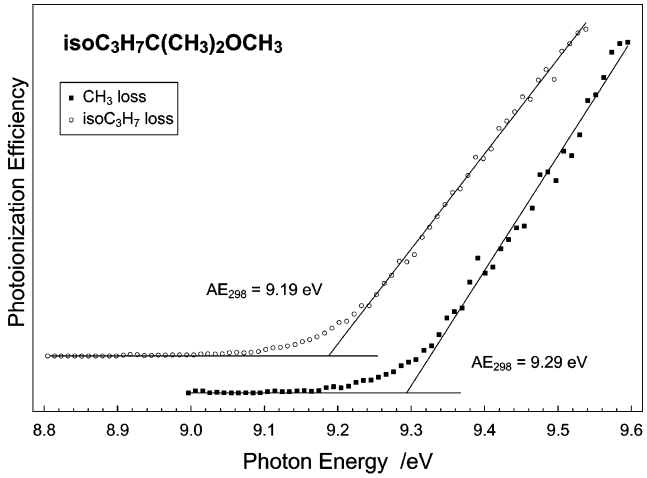

Figure 4. Photoionization efficiency curves near onset for loss of methyl radical (*m*/*z* 101) and for loss of C_3H_7 radical (*m*/*z* 73) from methyl *tert*-hexyl ether (**3**) showing 298 K appearance energies. The observed 298 K threshold for loss of propane is 9.06 eV.

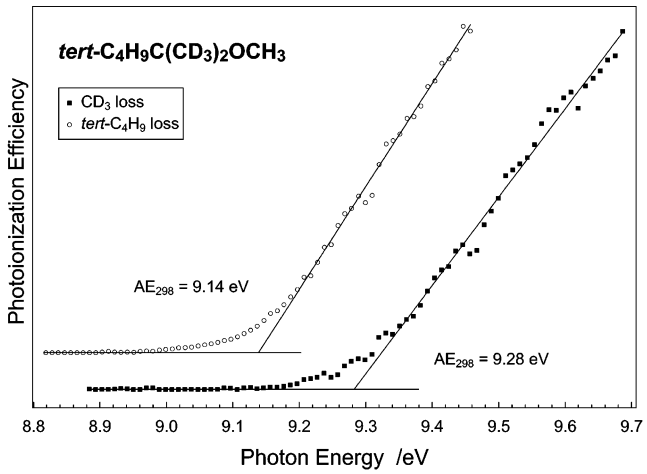

Figure 5. Photoionization efficiency curves near onset for loss of CD_3 radical (*m*/*z* 118) and for loss of C_4H_9 radical (*m*/*z* 79) from **4**-d_6 showing 298 K appearance energies. The 298 K thresholds for loss of C_4H_9D and for loss of CH_3 radical are 9.04 and 10.38 eV, respectively.

at 0 K) indicates that the CF_3 loss threshold represents the onset of ionization rather than a true AE.

In contrast to the foregoing examples, methyl radical losses from photoionization of ethers of the general formula $RC(CH_3)_2OCH_3$ have their onsets well above the thermodynamic threshold, as illustrated by the photoionization efficiency curves in Figures 2−6. For clarity, the figures omit the threshold behavior for alkane expulsions, which have lower AEs than do losses of the corresponding alkyl radicals. For instance, the AE for ethane expulsion from TAME (*m*/*z* 72) is 0.10 eV lower than the AE for loss of ethyl radical (*m*/*z* 73). It is therefore clear that the AEs for radical losses have values higher than the onset of ionization.

The AEs for R• radical loss are lower than for methyl loss, even though those cleavages are thermochemically less favorable, as Table 1 summarizes. The values of $\Delta H_{Me}^{\ddagger} - \Delta H_R^{\ddagger}$ are assessed, as Figure 1 depicts, as the sum of the difference in appearance energies (ΔAE) and the difference in G3 0 K heats of formation of the dissociation products ($\Delta\Delta H$). For R = isopropyl, $\Delta H_{Me}^{\ddagger} - \Delta H_R^{\ddagger}$ for the methyl ether turns out to be the same as for ionized 2,3-dimethyl-2-butanol (thexyl alcohol),[18] for which the difference in barrier heights (vide supra) equals 21 kJ mol^{-1}.

To confirm the origin of expelled methyl radicals, a variety of deuterated analogues were prepared and examined. Photoionization of $CH_2DCH_2C(CH_3)_2OCH_3$ (a monodeuterated analogue of TAME) below 12.5 eV showed loss of methyl and of monodeuterated ethyl radicals with the same appearance energies as seen for undeuterated TAME but no loss of CH_2D. By contrast, ethers with deuterated α-methyl groups, $(CH_3)_2CHC(CD_3)_2OCH_3$ and $(CH_3)_3CC(CD_3)_2OCH_3$, exhibited losses of CD_3 radicals with the same AE values as for CH_3 losses from the corresponding undeuterated analogues. In the latter ether, CH_3 loss (from the *tert*-butyl group) had an AE 0.8 eV higher than CD_3 loss. Finally, $(CH_3)_3CCH_2C(CH_3)_2OCD_3$, a trideuterated analogue of TOME, exhibited loss of CH_3 and no loss of CD_3 radical.

With regard to photoionization of the ethers, the magnitude of $\Delta H_R^{\ddagger}$ (eq 3) remains uncertain. The 0 K appearance energy for TAME is predicted to be 9.437 eV (G3) or 9.438 eV (G3B3), while the experimental value (determined by correcting the 298 K AE in Figure 1 for the thermal vibrational energy of neutral TAME) is 0.03 eV higher, as the first column in Table 1 summarizes. If G3 theory makes a correct prediction, then the comparison of experiment with theory yields a barrier for adding an ethyl radical to $(CH_3)_2C{=}OCH_3^+$ (R = ethyl in eq 3) of

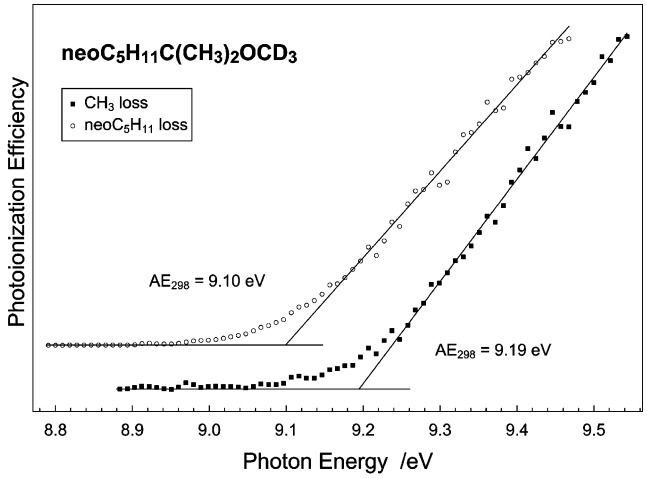

Figure 6. Photoionization efficiency curves near onset for loss of methyl radical (*m*/*z* 132) and for loss of C_5H_{11} radical (*m*/*z* 76) from **5**-d_3 showing 298 K appearance energies. The observed 298 K threshold for loss of C_5H_{12} is 8.97 eV.

$\Delta H_{Et}^{\ddagger} = 3$ kJ mol^{-1}. Given the accuracy of G3 theory and the experimental uncertainty of the AE measurement (± 1 kJ mol^{-1}), the experimental AE for ethyl loss does not definitively answer the question as to whether there is any barrier at all for the addition of larger radicals.

To explore this issue further, experimental AEs are compared for the expulsion of ethyl vs *n*-propyl radicals from ionization of ethers containing both ethyl and *n*-propyl groups. This competition was examined for *n*-PrCEt$_2$OMe (**6**) and *n*-PrC(CD$_3$)EtOMe (**7**). Both ethers exhibit thresholds for ethane loss and for propane loss below the onsets of radical expulsions. In the former ether, the 298 K AE for ethyl loss has a value 0.01 eV lower than for *n*-propyl loss. For the latter, the 298 K AE for ethyl loss has a value 0.02 eV lower than for *n*-propyl loss. Both G3 and G3B3 calculations predict that ethyl loss from ionization of the latter compound should be thermodynamically favored by between 5.5 and 6 kJ mol^{-1} over propyl loss. That is to say, the experimental AE difference is not as large as the thermodynamic value predicted by theory. On that basis (by analogy to Figure 1), one calculates the difference in barriers for addition of ethyl versus propyl as $\Delta H_{Et}^{\ddagger} - \Delta H_{nPr}^{\ddagger} = 4$ kJ mol^{-1}. Hence, there must be at least a small barrier for addition of ethyl radical to $(CH_3)_2C{=}OCH_3^+$.

In comparing losses of larger radicals, $\Delta H_{iPr}^{\ddagger} - \Delta H_{nPr}^{\ddagger}$ appears to be zero. Comparison of the appearance energies for 2-methoxy-2-methylpentane (**2**) and its branched isomer **3** suggests that these larger radicals do not encounter different activation barriers in adding to $Me_2C{=}OMe^+$. The most abundant fragment ion from both ethers arises via loss of C_3H_7 radical, an *n*-propyl radical in the former case and an isopropyl in the latter. The heats of formation of those two radicals differ by 10 ± 2 kJ mol^{-1},[19] and the isomeric ethers have heats of formation that differ by 6 kJ mol^{-1}. One should therefore expect the AEs for C_3H_7 radical loss to differ by $10 - 6 = 4$ kJ mol^{-1} if the ionization onsets correspond to thermodynamic thresholds. The experimental AEs differ by 3.5 kJ mol^{-1}.

Addition of methyl radical to the *O*-methylated 3-hexanone ion seems to behave differently from addition of methyl radical to the *O*-methylated 2-pentanone ion. The AE for loss of CD_3 from *n*-PrC(CD$_3$)EtOMe is the same as that for ethyl loss and is 0.02 eV lower than for propyl loss. Thermochemical calculations predict methyl loss to be 0.094 eV (at G3) or 0.075 eV (at G3B3) more favorable than propyl loss. The difference in barrier heights $\Delta H_{Me}^{\ddagger} - \Delta H_{nPr}^{\ddagger}$ is much smaller for this ether than for the examples listed in Table 1. This means that either $\Delta H_{nPr}^{\ddagger}$ has a greater value or that $\Delta H_{Me}^{\ddagger}$ has a smaller value than for ethers of the general formula $RC(CH_3)_2OCH_3$.

Discussion

Addition of a free radical R$^\bullet$ to the oxygen-stabilized ion $(CH_3)_2C{=}OCH_3^+$ is the reverse of the dissociation of the radical cations $RC(CH_3)_2OCH_3^{\bullet+}$. Since that radical cation can rarely be observed, inferences about potential energy barriers for the forward and reverse reactions must be drawn from appearance energy measurements of their dissociation fragments.

Mass spectrometry is the standard method for detecting *tert*-alkyl methyl ethers as environmental pollutants. Because these compounds are used as gasoline additives,[21] their mass spectra have been recorded many times. Electron ionization of molecules having the general structure $RC(CH_3)_2OCH_3$ shows the same base peak, *m*/*z* 73, regardless of the identity of the alkyl group R. In the case of MTBE (R$=$CH$_3$), this fragmentation corresponds to α-cleavage of a methyl radical, for which we[10] and others[9] have reported the photoionization threshold. In the case of TAME (R $=$ C$_2$H$_5$), *m*/*z* 73 corresponds to loss of an ethyl radical, which intuition (and, as noted in Table 1, theory) suggests is more endothermic than loss of methyl radical. Nevertheless, the 70-eV mass spectrum shows that loss of methyl radical from ionized TAME (*m*/*z* 88) gives a peak less than a quarter as intense as *m*/*z* 73.[19] Similarly, the mass spectrum of TOME (**5**, R $=$ (CH$_3$)$_3$CCH$_2$) also exhibits *m*/*z* 73 as its base peak, the fragment from α-cleavage of a neopentyl group.[10]

Isotopic labeling studies (e.g., using **3**-d_6 and **4**-d_6) confirm that the lighter ions do not come from dissociation of the heavier fragment ions. Hence, the observed intensity ratio reflects competition between two α-cleavage pathways. Other classes of compounds have been described, for which the competition favors cleavage of large neutrals more readily than smaller ones at high internal energies, despite the fact that the thermochemically more favorable cleavage of the smaller neutral predominates at low internal energies.[22] In the present work, however, *m*/*z* 73 has a greater abundance than heavier α-cleavage fragment ions at threshold and over the entire domain of photon energies investigated (up to 10.5 eV).

TABLE 1: Appearance Energies for Loss of R$^\bullet$ from Photoionized RCMe$_2$OMe Corrected to 0 K, Appearance Energy Differences (ΔAE) between Methyl Radical Loss and R$^\bullet$ Loss, G3 and G3B3 0 K Enthalpy Differences between Eqs 2 and 3 (ΔΔH), and the Resulting Difference in Activation Barriers for Addition of Radicals to *O*-Methylated Ketone Ions ($\Delta H_{Me}^{\ddagger} - \Delta H_R^{\ddagger} = \Delta AE + [\Delta\Delta H_{G3} + \Delta\Delta H_{G3B3}]/2$)

R	0 K $AE_{[M-R]^+}$	ΔAE	$\Delta\Delta H_{G3}$	$\Delta\Delta H_{G3B3}$	$\Delta H_{Me}^{\ddagger} - \Delta H_R^{\ddagger}$
ethyl (**1**)	9.47 eV	0.11 eV	0.100 eV[a]	0.086 eV[a]	19.6 ± 1.7 kJ mol^{-1}
n-propyl (**2**)	9.49 eV	0.09 eV	0.159 eV[a]	0.145 eV[a]	23.4 ± 1.7 kJ mol^{-1}
isopropyl (**3**)	9.45 eV	0.10 eV	0.118 eV	0.092 eV	19.8 ± 2.8 kJ mol^{-1}
tert-butyl (**4**-d_6)	9.43 eV	0.14 eV	0.115 eV[a]	0.087 eV[a]	23.3 ± 3.0 kJ mol^{-1}
neopentyl (**5**-d_3)	9.42 eV	0.09 eV	0.167 eV	0.153 eV[a]	24.2 ± 1.7 kJ mol^{-1}

[a] Ionic fragment from methyl loss has C_s symmetry.

Why do ethers of the general formula $RCMe_2OMe$ all give the same base peak? The combination of photoionization threshold measurements and calculations reported herein imply that expulsions of methyl radicals have to overcome a 20−24 kJ mol^{-1} energy maximum in excess of the thermochemical threshold, while larger radicals encounter much lower barriers. In other words, the addition of methyl radicals to oxygen-stabilized cations encounters higher barriers than does addition of radicals with ≥2 carbons, as portrayed by the qualitative curves drawn in Figure 1.

The $\Delta H_{Me}^{\ddagger} - \Delta H_R^{\ddagger}$ values summarized in Table 1 can be compared with the activation barrier for addition of a methyl radical to a neutral carbonyl group. Reported barriers for decomposition of the *tert*-butoxy radical lie in the range 57−64 kJ mol^{-1}.[23] This reaction is endothermic by only about 10 kJ mol^{-1}.[24] Subtracting the value of ΔH from this activation barrier gives a barrier for addition of methyl radical to acetone on the order of 50 ± 4 kJ mol^{-1}.

The C−O bond orders for oxygen-stabilized cations are close to $n = 1.5$ (as noted in the Experimental Section), compared with a bond order of $n = 2$ for simple ketones. At the same time, the barriers for addition of methyl radicals have values of $\Delta H_{Me}^{\ddagger}$ on the order of one-half the activation barrier for addition to a ketone (assuming that the values for $\Delta H_R^{\ddagger}$ are not much greater than 5 kJ mol^{-1}). Thus, it is tempting to infer a relationship between the C−O bond order and the activation barrier.

Photoionization results for tertiary alcohols contradict inferences that might be drawn from this naïve supposition. Replacing an *n*-alkyl group attached to a carbonyl with a trifluoromethyl group increases the C═O bond order, yet it decreases the experimental value of $\Delta H_{Me}^{\ddagger} - \Delta H_R^{\ddagger}$. Protonated trifluoromethyl ketones have DFT C═O bond orders of $n = 1.6$. In comparison of thexyl alcohol (^{i}PrCMe$_2$OH) with EtC(CF$_3$)-MeOH (trifluorinated *tert*-amyl alcohol), the value of $\Delta H_{Me}^{\ddagger} - \Delta H_{iPr}^{\ddagger}$ for ionization of the former is the same (within experimental error) as for the corresponding methyl ether (R = isopropyl in Table 1). By contrast, the value of $\Delta H_{Me}^{\ddagger} - \Delta H_{Et}^{\ddagger}$ cannot be greater than 5 kJ mol^{-1} for photoionization of the latter alcohol.

A more systematic model for activation barriers provides a qualititative interpretation of the appearance energies for fragments from the RC(CH$_3$)$_2$OCH$_3$ homologous series. Three sorts of effects are believed to modulate the barrier for adding a radical to a multiple bond: the exothermicity of the reaction, mixing with excited states, and charge-transfer electronic configurations.[25] The Configuration Mixing model put forth by Shaik[26] and Pross[27] (often called the curve-crossing model[24,28−30]) addresses these latter two contributions in terms of vertical energies. In regard to eq 3, the relevant excited state is the lowest triplet of the double bond in its ground-state geometry. The relevant charge transfer state corresponds to electron transfer from the radical R• to the cation. For neutral systems, two charge-transfer configurations need to be considered; however, for the cationic systems considered here, transferring an electron *to* the radical can be neglected, because it would correspond to removal of an electron from a cation.

Viewed from right to left, Figure 1 depicts the comparison between eqs 2 and 3. The experimental difference in barrier heights, $\Delta H_{Me}^{\ddagger} - \Delta H_R^{\ddagger}$, is substantially larger than the difference in exothermicity. The curve-crossing model asserts that relative barrier heights reflect the relative energies for charge transfer and of the vertical triplet states. This model for the origin of activation barriers makes a specific qualitative prediction: all other things being equal, the barrier height $\Delta H^{\ddagger}$ should become lower as the energies of the vertical triplet and the charge-transfer electronic configuration decrease relative to the ground electronic state. The net thermochemistry of the reaction must also play a role, but that is harder to gauge, since the radical cations cannot be observed. It remains to be seen if reliable energies for these molecular ions (and the transition states for their bond homolyses) can be calculated ab initio.

When radicals attack double bonds of neutral molecules, the calculated differences in barrier heights are smaller than the differences in net exothermicities.[24,25] In comparison of eqs 2 and 3, Table 1 shows that the differences in barrier heights, $\Delta H_{Me}^{\ddagger} - \Delta H_R^{\ddagger}$, are approximately twice as large as the differences in enthalpy changes. At the same time, however, the vertical ionization energies of the neutral radical decrease by at least 1.4 eV in going from methyl to larger alkyl groups.[31,32] That is to say, the energy of the charge-transfer electronic configuration drops substantially when $CH_3^{\bullet}$ is replaced by R• radicals containing > 2 carbon atoms. This interpretation suggests why $\Delta H_R^{\ddagger}$ values are lower when R is not methyl and provides a qualitative explanation as to why the barrier height $\Delta H_{Me}^{\ddagger}$ is so much larger.

The data in the right-hand column of Table 1 display no significant overall trend as the bulk of the R group increases. However, there are differences between isomeric systems, for which the curve crossing model provides a qualitative explanation. The value of $\Delta H_{Me}^{\ddagger} - \Delta H_{nPr}^{\ddagger}$ for 2-methoxy-2-methylpentane (**2**) is 3.6 ± 0.6 kJ mol^{-1} greater than the value of $\Delta H_{Me}^{\ddagger} - \Delta H_{iPr}^{\ddagger}$ for its branched isomer **3**. This is consistent with expectation: while DFT calculations give the same vertical neutralization energies for the two isomeric $C_3H_7C(CH_3)$═OCH_3^+ ions, the vertical triplet of the *n*-propyl isomer is calculated to lie 4.6 kJ mol^{-1} higher than that of the isopropyl isomer.

The curve-crossing model can account for trends in Table 1, but it is not easy to generalize more widely. As noted in the Introduction, ab initio calculations predict that there are no energy barriers in the addition of methyl radical to methyl, ethyl, or isopropyl carbocations. Likewise, the photoionization of 1,1,1-trifluoro-2-methyl-2-butanol, reported above (R = ethyl, X = F in eq 4), does not show evidence of a large barrier for adding methyl radical to EtC(CF$_3$)═OH$^+$, when compared with theory, even though published experiments[18] (and calculations presented here) do indicate a barrier of 22 kJ mol^{-1} for addition of methyl radical to iPrC(CH$_3$)═OH$^+$.

In the *O*-methyl compounds, the loss of methyl-d_3 vs ethyl radical from *n*-PrC(CD$_3$)EtOMe does not parallel the competition observed for *n*-PrC(CH$_3$)$_2$OMe: the barrier for adding methyl radical to *n*-PrCEt═OMe$^+$ is significantly lower than the barrier for addition to *n*-PrCMe═OMe$^+$. Whereas the barrier heights in Table 1 are all nearly the same and can be rationalized based on the difference in ionization energies between methyl and larger radicals, the deviation in barrier height in response to a comparatively subtle change in the substitution pattern of the ion (e.g., *n*-PrCEt═OMe$^+$ vs *n*-PrCMe═OMe$^+$) suggests that there is a great deal more to be learned regarding the factors that control activation energies.

Conclusions

The experiments described above demonstrate that cleavage of alkyl groups α to an ionized ether oxygen display a distinct energetic preference. When there are two methyls and one larger group, loss of the larger group occurs at a lower threshold energy, even though methyl loss is thermochemically more

favorable. This leads to the conclusion that the reverse activation barrier for methyl loss is at least 20 kJ mol^{-1} greater than for loss of a larger radical, i.e., that addition of a methyl radical to oxygen-stabilized cations of the general formula $CH_3CR{=}OCH_3^+$ encounters a substantially higher barrier than does addition of a radical with ≥2 carbon atoms. The curve-crossing model provides an explanation for this difference, in terms of mixing of excited electronic configurations.

There is no evidence that steric crowding affects the barrier height for methyl radical addition to $RCMe{=}OMe^+$ ions. That outcome is consistent with previously published calculations, which suggest the transition state to have a C−C distance ≥2 Å, quite elongated relative to the geometry of the ionized ether.[9] Sufficient data are now in hand to permit future theoretical explorations of these transition states and comparisons with experiment.

Acknowledgment. The authors are grateful to Jintao Zhang and to Prof. T. Keith Hollis for assistance with computation. This work was supported by NSF Grant CHE0316515.

Supporting Information Available: Calculated G3 and G3B3 0 K energies of photoionization fragments (Table 2) and first differential photoionization onset curve for 2,2-dimethylbutane (Figure 7). This material is available free of charge via the Internet at http://pubs.acs.org.

References and Notes

(1) Smith, G. P. *Chem. Phys. Lett.* **2003**, *376*, 381−388.

(2) Gräfenstein, J.; Kraka, E.; Cremer, D. *J. Chem. Phys.* **2004**, *120*, 524−539.

(3) (a) Olivella, S.; Solé, A.; McAdoo, D. J. *J. Am. Chem. Soc.* **1996**, *118*, 9368−9376. (b) McAdoo, D. J.; Olivella, S.; Solé, A. *J. Phys. Chem. A* **1998**, *102*, 10798−10804.

(4) Olivella, S.; Solé, A.; McAdoo, D. J.; Griffin, L. L. *J. Am. Chem. Soc.* **1994**, *116*, 11078−11088.

(5) (a) Mandelcorn, L.; Steacie, E. W. R. *Can. J. Chem.* **1954**, *32*, 474−484. (b) Landers, L. C.; Volman, D. C. *J. Am. Chem. Soc.* **1957**, *79*, 2996−2999. (c) Brinton, R. K. *J. Chem. Phys.* **1958**, *29*, 781−786.

(6) Slagle, I. R.; Batt, L.; Gmurczyk, G. W.; Gutman, D.; Tsang, W. *J. Phys. Chem.* **1991**, *95*, 7732−7739.

(7) Sun, H.; Bozelli, J. W. *J. Phys. Chem. A* **2004**, *104*, 1694−1711.

(8) Hammerum, S.; Derrick, P. J. *J. Chem. Soc., Chem. Commun.* **1985**, 996.

(9) Beveridge, W.; Hunter, J. A.; Johnson, C. A. F.; Parker, J. E. *Org. Mass Spectrom.* **1992**, *27*, 543−548.

(10) Chambreau, S. D.; Zhang, J.; Traeger, J. C.; Morton, T. H. *Int. J. Mass Spectrom.* **2000**, *199*, 1727.

(11) McBee, E. T.; Pierce, O. R.; Higgins. J. F. *J. Am. Chem. Soc.* **1952**, *74*, 1736−1737.

(12) Traeger, J. C. *Rapid Commun. Mass Spectrom.* **1996**, *10*, 119−122.

(13) Traeger, J. C.; Morton, T. H. *J. Am. Chem. Soc.* **1996**, *118*, 9661−9668.

(14) Harvey, Z. A.; Traeger, J. C. *J. Mass Spectrom.* **2004**, *39*, 802−807.

(15) (a) Curtiss, L. A.; Raghavachari, K.; Redfern, P. C.; Rassolov, V.; Pople, J. A. *J. Chem. Phys.* **1998**, *109*, 7764−7776. (b) Baboul, A. G.; Curtiss, L. A.; Redfern, P. C.; Raghavachari, K. *J. Chem. Phys.* **1999**, *110*, 77650−7657. (c) Curtiss, L. A.; Raghavachari, K.; Redfern, P. C.; Pople, J. A. *J. Chem. Phys.* **2000**, *112*, 7374−7383.

(16) (a) Hammerum, S. *Chem. Phys. Lett.* **1999**, *300*, 529−532. (b) Feng, Y.; Liu, L.; Wang, J.-T.; Zhao, S.-W.; Guo, Q.-X. *J. Org. Chem.* **2004**, *69*, 3129−3138.

(17) (a) Biegler-König, F. W.; Bader, R. F. W.; Tang, T. H. *J. Comput. Chem* **1982**, *3*, 317−328. (b) Biegler-König, F.; Schönbohm, J.; Bayles, D. *J. Comput. Chem.* **2001**, *22*, 545-559; Biegler-König, F. Schönbohm, J. *J. Comput. Chem.* **2002**, *23*, 1489−1494.

(18) Traeger, J. C.; Morton, T. H. *J. Am. Soc. Mass Spectrom.* **2004**, *15*, 989−997.

(19) NIST Chemistry Webbook (http://webbook.nist.gov/chemistry).

(20) Steiner, B.; Giese, C. F.; Inghram, M. G. *J. Chem. Phys.* **1961**, *34*, 189−220.

(21) *Oxygenates in Gasoline: Environmental Aspects*; Diaz, A. F., Drogos, D., Eds.; American Chemical Society: Washington, DC, 2002.

(22) Griffin, L. L.; Traeger, J. C.; Hudson, C. E.; McAdoo, D. J. *Int. J. Mass Spectrom.* **2002**, *217*, 23−44.

(23) (a) Blitz, M.; Pilling, M. J.; Robertson, S. H.; Seakins, P. W. *Phys. Chem. Chem. Phys.* **1999**, *1*, 73−80. (b) Park, J. M.; Song, N. W.; Choo, K. Y. *Bull. Korean Chem. Soc.* **1990**, *11*, 343−347. (c) Fittschen, C.; Hippler, H.; Viscolz, B. *Phys. Chem. Chem. Phys.* **2000**, *2*, 1677−1683.

(24) Rauk, A.; Boyd, R. J.; Boyd, S. L.; Henry, D. J.; Radom, L. *Can. J. Chem.* **2003**, *81*, 431−442.

(25) (a) Lalevée, J.; Allonas, X.; Fouassier, J.-P. *J. Phys. Chem. A* **2004**, *108*, 4326−4334. (b) Lalevée, J.; Allonas, X.; Fouassier, J.-P. *J. Org. Chem.* **2005**, *70*, 814−819.

(26) Shaik, S. *Prog. Phys. Org. Chem.* **1985**, *15*, 197−337.

(27) Pross, A. *Adv. Phys. Org. Chem.* **1985**, *21*, 99−196.

(28) Gómez-Balderas, R.; Coote, M. L.; Henry, D. J.; Fischer, H.; Radom, L. *J. Phys. Chem A* **2003**, *107*, 6082−6090.

(29) Gómez-Balderas, R.; Coote, M. L.; Henry, D. J.; Radom, L. *J. Phys. Chem A* **2004**, *108*, 2874−2883.

(30) Henry, D. J.; Coote, M. L.; Gómez-Balderas, R.; Radom, L. *J. Am. Chem. Soc.* **2004**, *126*, 1732−1740.

(31) Houle, F. A.; Beauchamp, J. L. *J. Am. Chem. Soc.* **1979**, *101*, 4067−4074.

(32) Schultz, J. C.; Houle, F. A.; Beauchamp, J. L. *J. Am. Chem. Soc.* **1984**, *106*, 3917−3927.